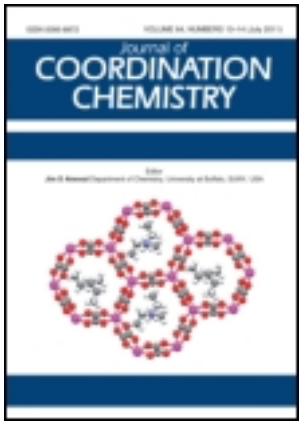

Journal of Coordination Chemistry
Publication details, including instructions for authors and subscription information:
http://www.tandfonline.com/loi/gcoo20

Crystal structures and proton conductivities of two molecular hybrids based on decorated poly-Keggin-anion chains

Meilin Wei [a], Huihua Li [a] & Guangjie He [b]
[a] College of Chemistry and Environmental Science, Henan Normal University, Xinxiang 453007, P.R. China
[b] Department of Chemistry, Xinxiang Medical University, Xinxiang 453003, P.R. China
Published online: 29 Nov 2011.

To cite this article: Meilin Wei, Huihua Li & Guangjie He (2011) Crystal structures and proton conductivities of two molecular hybrids based on decorated poly-Keggin-anion chains, Journal of Coordination Chemistry, 64:24, 4318-4333, DOI: 10.1080/00958972.2011.639068

To link to this article: http://dx.doi.org/10.1080/00958972.2011.639068

Journal of Coordination Chemistry
Vol. 64, No. 24, 20 December 2011, 4318–4333

Crystal structures and proton conductivities of two molecular hybrids based on decorated poly-Keggin-anion chains

MEILIN WEI*†, HUIHUA LI† and GUANGJIE HE‡

†College of Chemistry and Environmental Science, Henan Normal University, Xinxiang 453007, P.R. China
‡Department of Chemistry, Xinxiang Medical University, Xinxiang 453003, P.R. China

(*Received 30 September 2011; in final form 1 November 2011*)

Two proton-conductive molecular hybrid complexes, $\{[H(H_2O)_2][Sr(HINO)_4(H_2O)_7(PW_{12}O_{40})]\}_n$ (**1**) and $\{[H(H_2O)_2][Ca(HINO)_4(H_2O)_5(PW_{12}O_{40})]\}_n$ (**2**), were constructed by introducing alkaline-earth metal ions and $[PW_{12}O_{40}]^{3-}$ anions in the gallery of H-bonding networks based on isonicotinic acid N-oxide (HINO). Single-crystal X-ray diffraction analyses at 293 K reveal that both complexes crystallized in the orthorhombic space group *P*nnm, and presented the same 3-D hydrogen-bonded networks with large 1-D channels. Interestingly, HINOs not only constructed 1-D hydrogen-bonded chains, but also coordinated to alkaline-earth metal ions to form decorated poly-Keggin-anions. In addition, decorated poly-Keggin-anion chains are also formed in the 1-D channels. Thermogravimetric analyses show no weight loss in the temperature range 20–70°C, indicating that all water molecules in the unit structure are not easily lost below 70°C. Surprisingly, the proton conductivities of **1** and **2** at 85–100°C under 98% relative humidity conditions reached good proton conductivities of 10^{-3} S cm^{-1}.

Keywords: Polyoxometalates; Crystal structure; Supramolecular complex; Isonicotinic acid N-oxide; Proton conductivity

1. Introduction

Solid-state materials with proton conductivities have interest for transport dynamics and applications in fuel cells [1, 2]. Heteropolyacids (HPAs) and other inorganic or organic compounds [3, 4] have been studied and applied to electrochemical devices. Keggin-type HPAs, possessing a unique discrete ionic structure including heteropoly anions and countercations (H^+, H_3O^+, $H_5O_2^+$, etc), are widely known as proton-conducting electrolytes for low-temperature hydrogen–oxygen fuel cells [3, 5]. However, the application of HPAs is limited by the extreme sensitivity of their conductivity to the relative humidity (RH) and the temperature of the surrounding atmosphere [6]. To overcome these problems, various attempts have been made to immobilize HPAs in

*Corresponding author. Email: weimeilin@henannu.edu.cn

Journal of Coordination Chemistry
ISSN 0095-8972 print/ISSN 1029-0389 online © 2011 Taylor & Francis
http://dx.doi.org/10.1080/00958972.2011.639068

silica gel and to disperse it in an organically modified electrolyte membrane and organic/inorganic hybrid membranes [7, 8]. In addition, to enable fast ionic conduction in the hybrid materials, the molecular modification of organic ligands to inorganic structures of HPAs has been investigated [9]. For a long time, we have focused on proton conductivity of organic/inorganic complexes based on transition metal salts of HPAs dispersing in self-ordered hydrogen-bonding (H-bonding) networks [10]. We have extended our studies to alkaline-earth metal salts of HPAs, with the aim of finding solid conductors with good conductive characteristics which are less sensitive to surrounding conditions. Salts with large cations crystallize with fewer water molecules than the acids, and are more stable. In this work, we have succeeded in constructing two proton-conductive organic/inorganic complexes by introducing alkaline-earth metal ions and $[PW_{12}O_{40}]^{3-}$ in the gallery of H-bonding networks constructed by isonicotinic acid N-oxide (HINO). Here, we report their syntheses, crystal structures, and proton conductivities as a function of temperature.

2. Experimental

2.1. *Materials and measurements*

All organic solvents and materials used for the synthesis were of reagent grade and used without purification. α-$H_3PW_{12}O_{40} \cdot 6H_2O$ was prepared according to a literature method [11] and characterized by infrared (IR) spectra and thermogravimetric analysis. HINO was synthesized according to a literature method [12] and characterized by IR spectra. Elemental analyses (C, H, and N) were carried out on a Perkin-Elmer 240 C analyzer. Powder X-ray diffraction (XRD) was performed on a Bruker D8 Advance Instrument using Cu-Kα radiation and a fixed power source (40 kv, 40 mA). IR spectra were recorded on a VECTOR 22 Bruker spectrophotometer with KBr pellets from 400 to 4000 cm^{-1} at room temperature. TG analysis was performed on a Perkin-Elmer thermal analyzer under nitrogen atoms at a heating rate of 10°C min^{-1}. For an electrical conductivity study, powdered crystalline samples were compressed to 0.8–1.0 mm thickness and 12.0 mm diameter under a pressure of 12–14 MPa. Ac impedance spectroscopy measurement was performed on a chi660d (Shanghai chenhua) electrochemical impedance analyzer with copper electrodes [10, 13] (the purity of Cu is more than 99.8%) over the frequency range from 10^5 Hz to 10 Hz. Samples were placed in a temperature–humidity controlled chamber (GT-TH-64 Z, Dongwan Gaotian Corp.). The conductivity was calculated as $\sigma = (1/R) \times (h/S)$, where R is the resistance, h is the thickness, and S is the area of the tablet.

2.2. *Synthesis of* $\{[H(H_2O)_2][Sr(HINO)_4(H_2O)_7(PW_{12}O_{40})]\}_n$ *(1)*

To get suitable single crystals for XRD analyses, we synthesized the title complex on a small scale. The formation of HPA strontium salts was accomplished by neutralization of the acids. α-$H_3PW_{12}O_{40} \cdot 6H_2O$ (180 mg, 0.06 mmol) and adding $SrCl_2 \cdot 6H_2O$ (17 mg, 0.06 mmol) dissolved in water (4 mL). The solution was heated at 80°C in a water bath. White crystals were formed by cooling the saturated solution and slow evaporation at room temperature, and characterized by IR spectrum. A mixture of resulting HPA

strontium salts (90 mg, 0.03 mmol) and HINO (17 mg, 0.12 mmol) was dissolved in enough acetonitrile/water (1 : 1, v/v) solution. Finally, the solution was filtered and left to evaporate at room temperature. Four or five days later, white crystals were collected and dried in air after quickly being washed with water. Yield: 77 mg, 86% based on α-$H_3PW_{12}O_{40} \cdot 6H_2O$. Anal. Calcd for $C_{24}H_{39}N_4O_{61}SrW_{12}P$ (%): C, 7.82; H, 1.07; N, 1.52. Found (%): C, 7.71; H, 1.01; N, 1.43. IR (KBr) ν, cm^{-1}: four characteristic vibrations resulting from heteropolyanions with the Keggin structure: 813 ν(W–Oc), 896 ν(W–Ob), 981 ν(W=Ot), 1081 ν(P–Oa); and another vibrations resulting from the HINO molecules: 3326 ν(O–H), 1704 ν(C=O), 1618 ν(C=C), 1280 ν(N–O), 1172 δ(C−H, in plane). The synthesis can be conducted using larger quantities and is reproducible. α-$H_3PW_{12}O_{40} \cdot 6H_2O$ (1800 mg, 0.6 mmol) and adding $SrCl_2 \cdot 6H_2O$ (161 mg, 0.6 mmol) dissolved in water (40 mL). The solution was heated at 80°C in a water bath. White crystals were formed by cooling the saturated solution and slow evaporation at room temperature. A mixture of resulting HPA strontium salts (1200 mg, 0.03 mmol) and HINO (223 mg, 0.12 mmol) dissolved in enough acetonitrile/water (1 : 1, v/v) solution was filtered and left to evaporate at room temperature. One or two days later, white crystals were collected and dried in air after quickly being washed with water.

2.3. *Synthesis of {[H(H$_2$O)$_2$][Ca(HINO)$_4$ (H$_2$O)$_5$(PW$_{12}$O$_{40}$)]} (2)*

Complex **2** was prepared on a small scale as for **1**, except using $CaCl_2$ (7 mg, 0.06 mmol) to replace $SrCl_2 \cdot 6H_2O$ Yield: 76.5 mg, 85% based on α-$H_3PW_{12}O_{40} \cdot 6H_2O$. Anal. Calcd for $C_{24}H_{35}N_4O_{59}CaW_{12}P$ (%): C, 8.00; H, 0.98; N, 1.56. Found (%): C, 7.88; H, 0.91; N, 1.47. IR (KBr) ν, cm^{-1}: four characteristic vibrations resulting from heteropolyanions with the Keggin structure: 813 ν(W–Oc), 896 ν(W–Ob), 981 ν(W=Ot), 1081 ν(P–Oa); and another vibrations resulting from the HINO molecules: 3326 ν(O–H), 1704 ν(C=O), 1618 ν(C=C), 1280 ν(N–O), 1172 δ(C−H, in plane). The synthesis can be conducted using larger quantities and is reproducible. Complex **2** was synthesized on a big scale in the same way as for **1**, except using $CaCl_2$ (67 mg, 0.6 mmol) to replace $SrCl_2 \cdot 6H_2O$.

2.4. *Crystal structure and determination*

Intensity data of **1** and **2** were collected on a Siemens SMART-CCD diffractometer with graphite-monochromated Mo-Kα radiation ($\lambda = 0.71073$) using SMART and SAINT [14]. The structure was solved by direct methods and refined on F^2 by using the full-matrix least-squares method with SHELXTL version 5.1 [15]. For **1** and **2**, all non-hydrogen atoms except some disordered oxygen atoms of polyanions and water were refined anisotropically. Hydrogen atoms of organic molecules were localized in their calculated positions and refined using a riding model. Hydrogen atoms of water molecule were not treated. The crystal parameters, data collection, and refinement results for both complexes are summarized in table 1. The selected bond lengths and angles are listed in table 2. Hydrogen-bond parameters are listed in table 3.

Table 1. Crystallographic data and refinement parameters for **1** and **2**.

	1	**2**
Empirical formula	$C_{24}H_{39}N_4O_{61}SrPW_{12}$	$C_{24}H_{35}N_4O_{59}CaPW_{12}$
Molecular weight	3684.38	3600.81
Crystal system	Orthorhombic	Orthorhombic
Space group	*P*nnm	*P*nnm
Unit cell dimensions (Å)		
a	10.474(10)	10.407(4)
b	15.770(15)	15.894(5)
c	19.327(19)	19.417(7)
Volume (Å^3), *Z*	3192(5), 2	3211.7(19), 2
Calculated density (g cm^{-3})	3.833	3.723
μ (mm^{-1})	22.502	21.621
F(000)	3280	3204
Reflections measured	14,965	15,014
Reflections unique	2907	2922
R_{int}	0.1705	0.0721
Refinement parameters	244	242
Goodness-of-fit on F^2	0.982	1.020
R_1/wR_2 [$I \geq 2\sigma(I)$]	0.0705/0.1550	0.0509/0.1359
R_1/wR_2 (all data)	0.0964/0.1609	0.0747/1.020
$\Delta\rho_{(max)}$ and $\Delta\rho_{(min)}$ (e Å^{-3})	3.687 and –4.377	3.395 and –2.131

Table 2. Selected bond lengths (Å) and angles (°) for **1** and **2**.

Complex **1**					
W(1)–O(5)	1.650(10)	Sr(1)–O(4 W)	2.246(14)	O(8)–W(1)–O(1)#1	64.9(5)
W(1)–O(4)	1.887(5)	Sr(1)–O(2 W)	2.43(3)	O(7)#4–W(1)–O(2)	91.6(5)
W(1)–O(7)#1	1.902(11)	Sr(1)–O(16)	2.624(11)	O(6)–W(1)–O(2)	64.2(6)
W(1)–O(8)	1.936(11)	Sr(1)–O(3 W)	2.632(13)	O(2 W)–Sr(1)–O(16)	77.9(3)
W(1)–O(6)	1.940(11)	Sr(1)–O(1 W)	2.720(19)	O(16)–Sr(1)–O(3 W)	71.7(5)
W(1)–O(1)#1	2.510(15)	O(4)–W(1)–O(8)	88.8(5)	O(3 W)–Sr(1)–O(3 W)#1	75.2(7)
W(1)–O(2)	2.524(15)	O(7)#1–W(1)–O(8)	86.8(5)	O(16)–Sr(1)–O(1 W)	93.1(3)
P(1)–O(3)	1.45(2)	O(5)–W(1)–O(10)	85.7(3)	O(3 W)–Sr(1)–O(1 W)	92.0(3)
P(1)–O(2)	1.47(2)	O(4)–W(1)–O(6)	86.6(5)	O(2 W)–Sr(1)–O(9)	87.4(9)
P(1)–O(1)	1.521(15)	O(7)#1–W(1)–O(6)	88.4(5)	O(16)–Sr(1)–O(9)	74.2(3)
Complex **2**					
W(1)–O(7)	1.652(7)	Ca(1)–O(3 W)	2.25(4)	O(10)–W(1)–O(1)#3	93.7(5)
W(1)–O(5)	1.884(9)	Ca(1)–O(2 W)	2.63(3)	O(8)#1–W(1)–O(3)	93.9(4)
W(1)–O(8)#2	1.892(8)	Ca(1)–O(16)#4	2.721(12)	O(4)–W(1)–O(3)	93.4(5)
W(1)–O(4)	1.892(5)	Ca(1)–O(1 W)	2.95(2)	O(2 W)–Ca(1)–O(2 W)#4	73.5(12)
W(1)–O(10)	1.924(8)	Ca(1)–O(3 W)	2.25(4)	O(3 W)–Ca(1)–O(16)	80.2(5)
W(1)–O(1)#3	2.460(13)	O(5)–W(1)–O(8)#2	88.8(4)	O(2 W)–Ca(1)–O(16)	70.9(6)
W(1)–O(3)	2.507(12)	O(8)#2–W(1)–O(4)	87.6(4)	O(3 W)–Ca(1)–O(9)	89.5(11)
P(1)–O(2)	1.465(18)	O(5)–W(1)–O(10)	85.7(3)	O(16)–Ca(1)–O(9)	74.9(3)
P(1)–O(3)	1.534(12)	O(4)–W(1)–O(10)	88.0(5)	O(2 W)–Ca(1)–O(1 W)	79.0(7)
P(1)–O(1)	1.557(19)	O(5)–W(1)–O(1)#3	93.4(4)	O(16)–Ca(1)–O(1 W)	90.3(4)

#1: $-x+1, -y+1, -z+1$; #2: $-x+2, -y+2, z$; #3: $-x+2, -y+2, -z+1$; #4: $x, y, -z+1$.

3. Results and discussion

3.1. *IR spectra*

IR spectra of both complexes are practically identical in shape and positions of their vibrational bands. The IR spectrum of HINO exhibits bands from 3060 to 1850 cm^{-1}

Table 3. Selected hydrogen bond lengths (Å) for **1** and **2**.

D···A	*d*(D···A)	Symmetry
Complex **1**		
O(17)···O(15)	2.510	$-x, -y-1, -z$
O(1 W)···O(5 W)	2.871	$-x, -y-1, z+1$
O(2 W)···O(6 W)	2.755	$-x, -y-1, -z$
O(3 W)···O(14)	2.632	
O(5 W)···O(13)	3.044	$-x+1, -y, z+1$
O(6 W)···O(5 W)	2.584	$-x, -y, -z$
O(6 W)···O(15)	2.652	
Complex **2**		
O(17)···O(15)	2.565	$-x+1, -y-1, -z$
O(1 W)···O(5 W)	2.595	$-x, -y-1, -z$
O(2 W)···O(6)	2.969	$-x+1, -y-1, -z$
O(2 W)···O(5 W)	3.027	$-x, -y-1, -z$
O(3 W)···O(5 W)	3.102	$x+1, y+2, -z+1$
O(4 W)···O(15)	2.772	
O(4 W)···O(3 W)	3.067	$-x+1, -y, -z$

due to hydrogen bonds (H···O–H), replaced in complexes by a strong and broad band with several peaks at 3500–3000 cm^{-1}, originating from extensive hydrogen-bonded lattice and aqua molecules. Comparison of these spectra shows that the ν(C=O) band at 1710 cm^{-1} in free HINO remains in similar position in the complexes, and a band due to antisymmetric COO^- stretch mode around 1640 cm^{-1} is not observed, indicating that COOH groups remain in these complexes. The ν(N–O) band at 1280 cm^{-1} remains in similar position in the complexes [10, 16]. The IR spectroscopic studies show that there are no strong interactions between the metal ions and the organic groups in the solid state. The proton polarizabilities are particularly large in the case of hydrogen-bonded chains because in such chains a collective proton-tunneling occurs. In FT-IR spectra, these hydrogen bonds or hydrogen-bonded chains are manifested as continua because they interact very strongly with their environments because of large proton polarizabilities, and vice versa, hydrogen bonds and hydrogen-bonded chains with large proton polarizabilities are indicated by these IR continua. Thus, such hydrogen-bonded chains are very effective proton pathways [17]. Water molecules are highly ordered for entropic reasons if they are in a hydrophobic environment. Therefore, they build up a particularly stable pathway. These IR continua indicate that these systems show proton polarizability due to collective proton motion.

3.2. *Structure description*

Complexes **1** and **2** were synthesized by the reaction of $MHPW_{12}O_{40} \cdot nH_2O$ and HINO at room temperature and characterized by single-crystal XRD, IR spectroscopy, TG and elemental analyses. XRD analyses at 293 K revealed that both complexes crystallized in the orthorhombic space group *P*nnm, exhibited very close unit cell parameters, and then presented 3-D H-bonding networks with large 1-D channels. Polyoxometalates (POMs) present a wide range of intriguing topologies and structures, with spherical surfaces giving an opportunity for forming coordination bonds or hydrogen bonds with organic or inorganic moieties [10]. Representative examples

include $(C_6H_{13}N_4)_2(H_3O)[Ce(H_2O)_5Mo_7O_{24}]\cdot 4H_2O$ [10i], $[Co(bipy)_3]_3[\{Co(bipy)_2(H_2O)\}_2\{H_3W_{12}O_{40}\}_2]\cdot H_2O$, and $[H_2bipy]_{0.5}[\{Cu(bipy)_2\}_2\{H_3W_{12}O_{40}\}]\cdot H_2O$ (bipy = 2,2′-pyridine) [10j]. Interestingly, in the title complexes, $[PW_{12}O_{40}]^{3-}$ anions form coordination bonds and hydrogen bonds with organic or inorganic moieties.

Complex **1** exhibited a 3-D H-bonding network with large 1-D channels constructed by HINO molecules, decorated Keggin-type $[Sr(HINO)_4(H_2O)_7(PW_{12}O_{40})]^-$ anions (figure 1), and $H^+(H_2O)_2$ clusters. In decorated Keggin-type $[Sr(HINO)_4(H_2O)_7(PW_{12}O_{40})]^-$, two halves of crystallographically identical Sr^{2+} are located symmetrically at opposite sites of the polyanion, and both connect with the terminal oxygen atoms of the polyanion, featuring Sr···Sr separation of 15.76 Å. Each half of Sr^{2+} is eight-coordinate by one oxygen atom (O(9)) from polyanion (Sr–O separation 2.796(2) Å), five oxygen atoms (O(1 W), O(2 W), O(3 W), O(3WA) O(4 W)) from water (mean Sr–O separation 2.531(4) Å), and two oxygen atoms (O(16), O(16 A)) from HINO molecules (mean Sr–O separation 2.624(6) Å). A terminal O(9) of the polyanion serves as a μ-2-oxo bridge to connect the polyanions with the Sr^{2+}. In other words, each $[PW_{12}O_{40}]^{3-}$ is coordinately bound to two $[Sr_{0.5}(HINO)_2(H_2O)_{3.5}]^+$ units by W–Ot–Sr bridges. As shown in figure 2, these decorated Keggin anions parallely arrange to form an infinite decorated poly-anion chain along the *a*-axis. In the polymeric polyanion, there are some short atom···atom separations of 3.13(2) Å, such as O(7B)···O(8BA), O(8B)···O(7BA), O(7AB)···O(8CA), and O(7CA)···O(8AB). Interestingly, as shown in figure 3, decorated poly-Keggin-anion chains are linked by small $H^+(H_2O)_2$ clusters into a 3-D network with large 1-D channels through hydrogen bonds between coordination water molecules (O(4 W), O(2 W) and O(1 W)) and water molecules (O(5 W) and O(6 W)) of small $H^+(H_2O)_2$ clusters, between oxygen atoms O(15) of

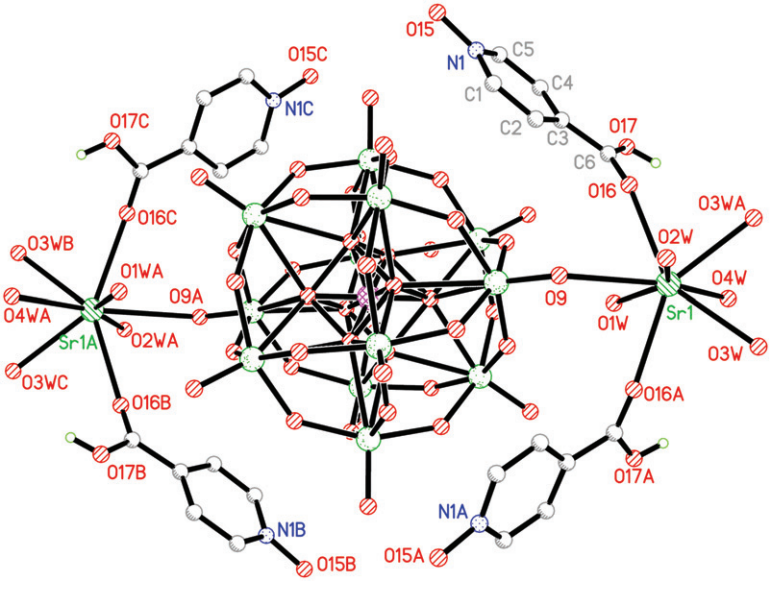

Figure 1. View of decorated Keggin-type $[Sr(HINO)_4(H_2O)_7(PW_{12}O_{40})]^-$ anions. Hydrogen atoms are omitted for clarity.

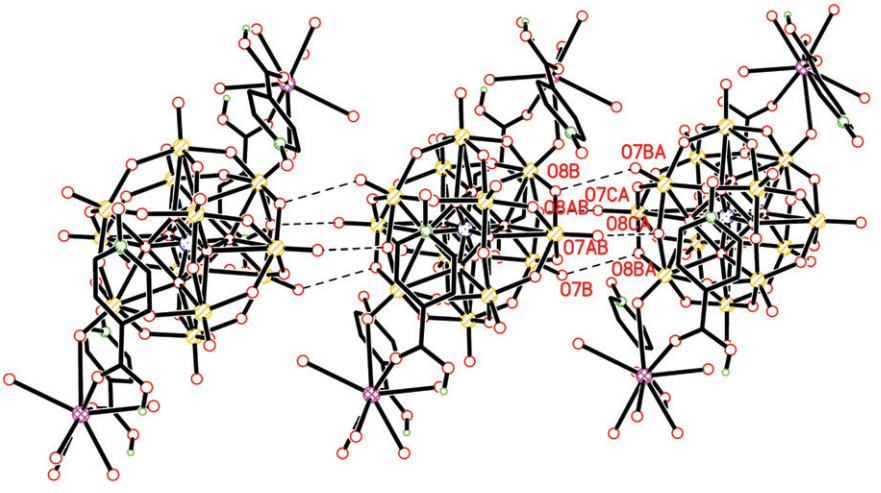

Figure 2. View of the 1-D decorated poly-anion chain $[Sr(HINO)_4(H_2O)_7(PW_{12}O_{40})]_n^{n-}$ along the *a*-axis. Hydrogen atoms are omitted for clarity.

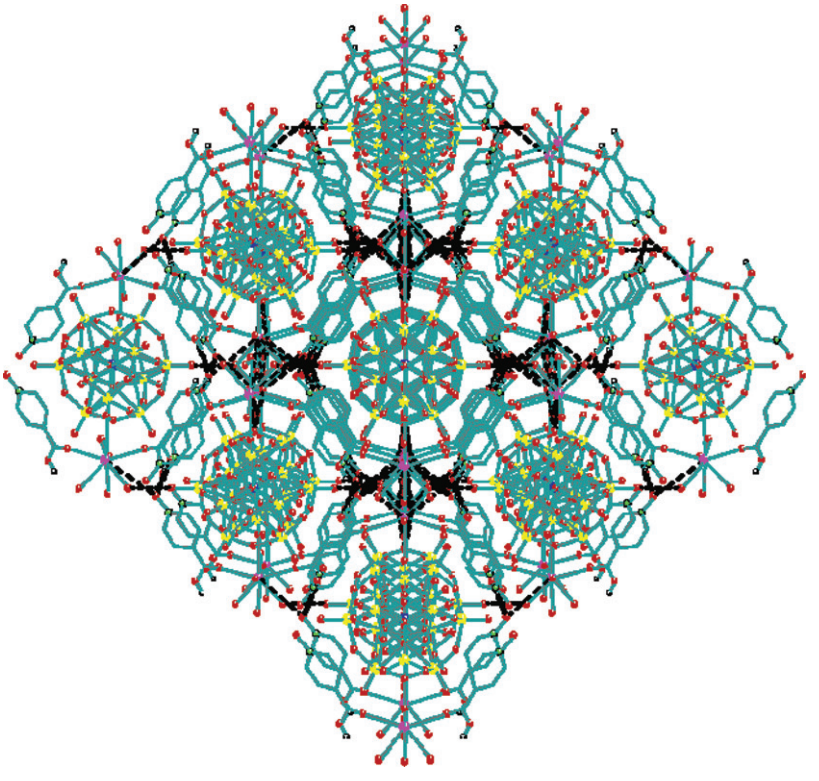

Figure 3. The 3-D hydrogen-bonded network in **1** showing the 1-D channels filled by decorated poly-Keggin-anion chains down the *a*-axis. Sr, N, O, W, and P are represented as purple, green, red, yellow, and blue, respectively. Hydrogen atoms are omitted for clarity.

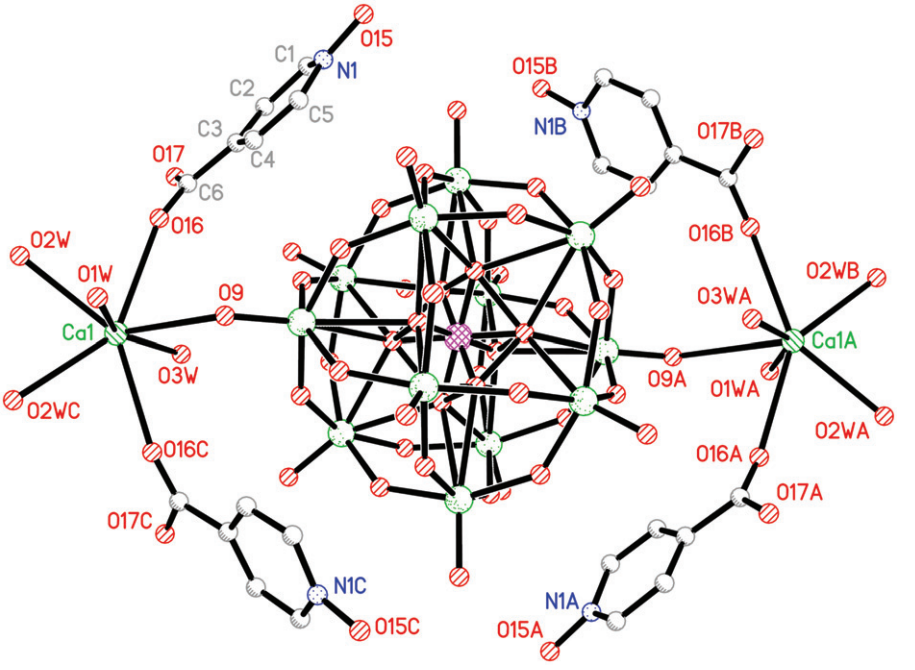

Figure 4. View of decorated Keggin-type $[Ca(HINO)_4(H_2O)_5(PW_{12}O_{40})]]^-$ anions. Hydrogen atoms are omitted for clarity.

HINO molecules and water molecule O(6 W) of small $H^+(H_2O)_2$ clusters, and between coordinated water molecule O(3 W) and oxygen atom O(14) of polyanions.

Complex **2** also presented a 3-D H-bonding network with large 1-D channels constructed by HINO molecules, decorated Keggin-type $[Ca(HINO)_4(H_2O)_5(PW_{12}O_{40})]^-$ anions (figure 4) and solvent water molecule. In decorated Keggin-type $[Ca(HINO)_4(H_2O)_5(PW_{12}O_{40})]^-$, two halves of crystallographically identical Ca^{2+} ions are located symmetrically at opposite sites of the polyanion, and both connect with terminal oxygen atoms of the polyanion, featuring the Ca···Ca separation of 15.89 Å. Each half of Ca^{2+} is seven-coordinate by one oxygen atom (O(9)) from polyanion (Ca–O separation 2.878(12) Å), four oxygen atoms (O(1 W), O(2 W), O(3 W), O(2WC)) from water molecules (mean Ca–O separation 2.655(4) Å), and two oxygen atoms (O(16), O(16 A)) from HINO molecules (mean Ca–O separation 2.721(12) Å). Terminal O(9) of the polyanion serves as a μ-2-oxo bridge to connect the polyanions with Ca^{2+}. Each $[PW_{12}O_{40}]^{3-}$ is coordinately bound to two $[Ca_{0.5}(HINO)_2(H_2O)_{2.5}]^+$ units by W–Ot–Ca bridges. Just like decorated Keggin-type $[Sr(HINO)_4(H_2O)_7(PW_{12}O_{40})]^-$ in **1**, decorated Keggin-type $[Ca(HINO)_4(H_2O)_5(PW_{12}O_{40})]^-$ is also parallely arranged to form an infinite decorated poly-anion chain along the *a*-axis. In the polymeric polyanion, there are some short atom···atom separations of 3.107(2) Å, such as O(7 A)···O(8BB), O(8 A)···O(7BB), O(7AA)···O(8CB) and O(7CB)···O(8AA). In addition, decorated poly-Keggin-anion chains are linked into a 3-D network with large 1-D channels through hydrogen bonds between coordination water molecules (O(1 W), O(2 W) and O(3 W)) and solvent water molecules (O(5 W) and O(4 W)), between oxygen

atoms O(15) of HINO molecules and water molecule O(4 W), and between coordinated water molecule O(2 W) and oxygen atom O(6) of polyanions.

As shown in figure 3, in both complexes, HINO molecules not only form H-bonding chains along the *b*-axis through O(15) of N–O and O(17) of O–H, but also bond to Sr^{2+} and Ca^{2+} by oxygen atom O(16) of the C=O as monodentate ligands [16]. These results suggested that COOH groups remain in the complexes and are in agreement with the results of IR studies.

In **1**, the section size of the channels based on the Sr···Sr separations is *ca* $10.5 \times 15.8 \times 19.3$ Å (these separations are almost equal to three axial lengths, respectively); in **2**, the section size of the channels based on the Ca···Ca separations is *ca* $10.5 \times 15.8 \times 19.4$ Å (these separations are almost equal to three axial lengths, respectively). These results indicate that each pore in the complexes could only accommodate a single Keggin anion. Interestingly, because the presence of positively charged species, $[Sr(HINO)_4(H_2O)_7]^{2+}$ and $[Ca(HINO)_4(H_2O)_5]^{2+}$, could attract polyanions, the Sr···Sr and Ca···Ca separations in the decorated poly-anion chains along the *a*-axis are much shorter than those separations along the *b* and *c* axes, resulting in each cavity being heavily condensed along the *a*-axis.

In the $[PW_{12}O_{40}]^{3-}$ units of the complexes, the central phosphorus is surrounded by a cube of eight oxygen atoms with each oxygen atom site half-occupied. These eight oxygen atoms are all crystallographically disordered, as found in many compounds [4, 10]. In **1**, the bond lengths of P–O and W–O are 1.45(2)–1.521(15) and 1.636(14)–2.524(15) Å, respectively; in **2**, the P–O and W–O bond lengths are 1.465(18)–1.557(19) and 1.650(10)–2.507(12) Å, respectively. The P–O and W–O bond lengths in the complexes are comparable to those in the 3-D porous polyoxometalate-based organic–inorganic hybrid materials with Keggin anions as guests [10]. In addition, the O–P–O angles are in the range 107.7(7)–112.2(12)° for **1** and 107.7(5)–111.0(9)° for **2**. All these results indicate that the $[PW_{12}O_{40}]^{3-}$ units have a normal Keggin structure in the polymeric-polyanion chains. The poly-Keggin-type anions play a charge-compensating role and can dramatically influence the overall solid-state architecture through their templating function, as well as the cationic framework with special channels also influencing the polymerization of polyanions through its host function. As a result, based on self-assembly of HINO molecules and $MHPW_{12}O_{40} \cdot nH_2O$, both complexes form 3-D H-bonding networks with 1-D channels along the *a*-axis, in which polyanion chains were formed and stabilized based on electrostatic and H-bonding interactions, resulting in $[PW_{12}O_{40}]^{3-}$ being not easily dissociated from the hybrid networks. Moreover, in each complex, the section size of the channels along the *b* and *c* axes is so much larger than the diameter of the $[PW_{12}O_{40}]^{3-}$ anion (*ca* 10.5 Å) that there is enough space outside the polyanion chains to admit some small species, such as water molecules or hydronium ions, to transport along the channels. All these results indicate that these complexes can potentially be good proton-conducting materials.

It is far more difficult to experimentally establish the position of excess proton unambiguously for such a complex system, since the presence of C–H vibrations of the ligand and solvent molecules, and the P–O, W–O vibrations of the anions all influence the observation of IR signals of O–H vibrations related to the excess proton. XRD analyses at 293 K revealed that **1** and **2** crystallize in the orthorhombic space group *P*nnm. Though the basic structure of the water cluster can be determined easily according to the result of the X-ray structure analysis, the X-ray structure is not refined at a level that can isolate the position of hydrogen atoms, and therefore cannot identify

the position of the proton. The determination of the protonated water is based on the stoichiometry, the crystal data, and relative references. It was reported that based on high-resolution solid-state ^{1}H and ^{31}P NMR, there were at least three different states for protons of $H_3PW_{12}O_{40} \cdot nH_2O$: (i) protons present in highly hydrated samples, (ii) protonated water which is hydrogen-bonded to terminal oxygen, $W=O \cdots H^+(H_2O)_2$ ($n=6$), and (iii) proton which is directly bonded to bridging oxygen, W–OH–W ($n=0$) [18a]. More recently, it was reported that based on REDOR experiments acidic protons are localized on both bridging (O_c) and terminal (O_d) oxygen atoms of the Keggin unit in the anhydrous state of $H_3PW_{12}O_{40}$ [18b]. In **1** and **2**, there are two lattice water molecules, so, we think that the excess proton is not localized on the surface of the polyanion, but in hydrated samples [10].

3.3. *TG analyses*

The Sr– and Ca–salts of tungstophosphoric acid and HINO are easily soluble in water, while the title complexes are slightly soluble in water. Water retention in the hybrid at high temperature is a key factor for having fast protonic conduction. TG analyses of the powder of the crystalline samples of the complexes in an atmosphere of N_2 (figure 5) show no weight loss in the temperature range 20–70°C, indicating that all water molecules in the unit structures are involved in constructing the H-bonding network, consistent with the structural analyses, and are not easily lost below 70°C. This is not like that observed in the proton conductors, including the quasi-liquid water clusters (which are generally loosely bonded in the structure) like a Nafion membrane [19] and pure tungstophosphoric acid (PWA-26) or molybdophosphoric acid (PMA-26) [3, 6]. All these results also indicate that **1** and **2** can potentially be proton-conducting material.

3.4. *Proton conductivity*

The proton conductivities of **1** and **2** in the temperature range 25–100°C were therefore evaluated by the ac impedance method using a compacted pellet of the powdered crystalline sample, which has the same structure as the single crystal (figure 6). At 25°C, both complexes showed poor proton conductivities of $1.9–6.7 \times 10^{-6}$ S cm^{-1} under 98% RH conditions, estimated from the Nyquist plots, but their proton conductivities reached $\sim 2.0 \times 10^{-3}$ S cm^{-1} with temperatures up to 100°C; both complexes reached high proton conductivities of $1.0–2.1 \times 10^{-3}$ S cm^{-1} at 85–100°C. Figure 7 shows the Arrhenius plots of the proton conductivities of the complexes from 25 to 100°C under 98% RH conditions. The $\ln\sigma T$ increases almost linearly with temperature range from 25 to 100°C, and the corresponding activation energy (E_a) of conductivity was estimated to be 0.86 eV for **1** and 0.87 eV for **2** from the equation below [10].

$$\sigma T = \sigma_0 \exp(-E_a/k_B T), \tag{1}$$

where σ is the ionic conductivity, σ_0 is the pre-exponential factor, k_B is the Boltzmann constant, and T is the temperature. Both E_a values are high in the temperature range 25–100°C. The results show that the general features of the changes in conductivities are different from those of proton-conducting polymer membrane such as Nafion, which

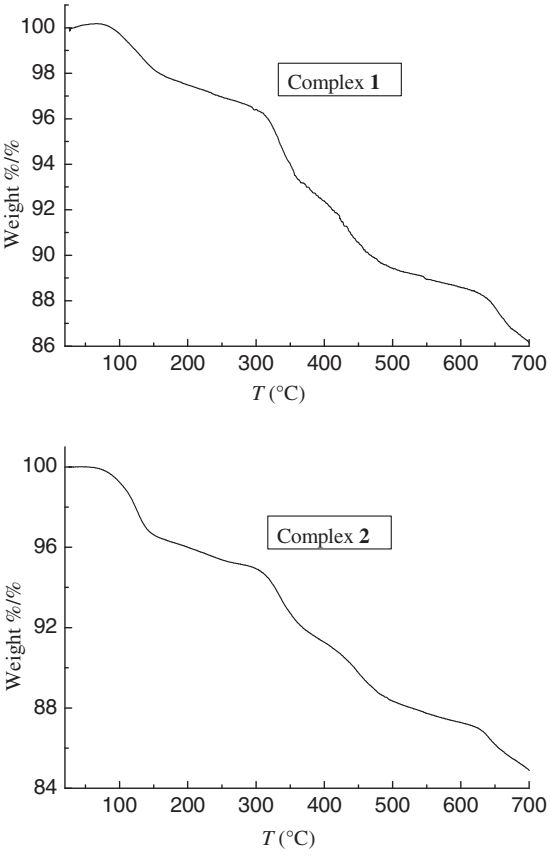

Figure 5. The curves of the TG analyses of **1** and **2** under N_2.

has almost identical protonic conductivity over a wide temperature range from ambient to 100°C with activation enthalpy of approximately 0.15 eV, when it is fully humidified [19], and are different from that of PWA-26 or PMA-26, whose proton conductivity decreased with temperature from ambient to 60°C [10]. However, the title complexes have thermally activated protonic conductivities [18b] from 25°C to 100°C; as the temperature increases, the proton conductivities increase on a logarithmic scale even with almost saturated humidities. This is probably due to the fact that protons belong to the protonated water clusters and those originating from water molecules need a thermally activated process for dissociation as hydrated forms such as H^+, H_3O^+, or other proton species at a distance from $[PW_{12}O_{40}]^{3-}$ clusters [20]. The mechanism of proton conduction of **1** and **2** is, therefore, expected to be similar to that of the vehicle mechanism [21], that is, the direct diffusion of additional protons with water molecules. As shown in figure 3, the section size of the channels along the *b* and *c* axes is larger than the diameter of the $[PW_{12}O_{40}]^{3-}$ anion (*ca* 10.5 Å), such that there is enough space outside the polyanion chains to admit some small species, such as water or hydronium ions, to transport along the channels. In addition, the existence of H-bonding networks [22] suggests that proton conduction includes some other process such as

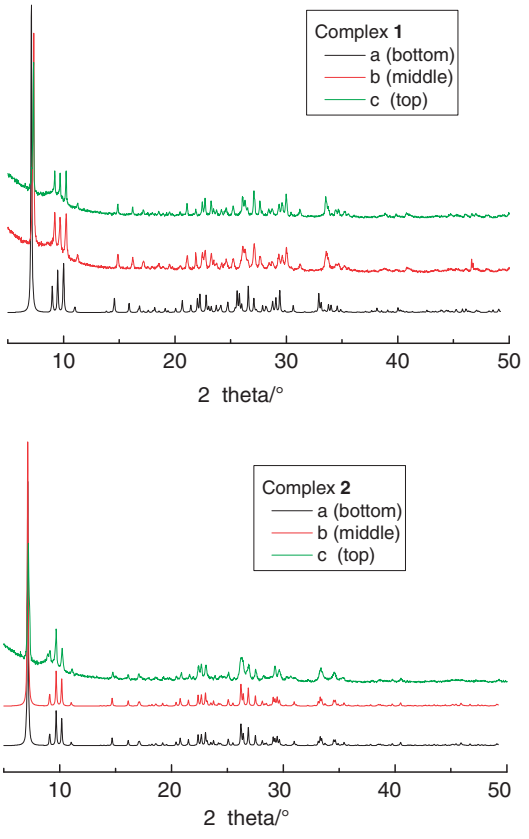

Figure 6. The powder XRD data of **1** and **2**; the simulated powder pattern (a), the powder before the proton-conductive measurement (b), and the powder after the proton-conductive measurement (c).

proton transport of additional protons along H-bonding networks (Grotthus mechanism) [23].

It is possible that in higher temperature and humidity some isonicotinic acid N-oxide molecules can be deprotonated and the protons can be incorporated by the water molecules and therefore conductivity can be a result of dissociation of organic acid. The results of measurement of the proton conductivity of HINO molecules in the temperature range 85–100°C at 98% RH showed that free HINO molecules reached proton conductivities of 10^{-5}–10^{-4} S cm^{-1} in the temperature range 85–100°C, about 1–2 orders of magnitude lower than that of the title complexes, which shows conductivity of about 10^{-3} S cm^{-1} in the conditions described. Therefore, the fact that **1** and **2** exhibit good proton conductivities in the temperature range 85–100°C is indicative of a high carrier concentration based on a thermally activated process, as well as the existence of H-bonding networks. Moreover, there is the possibility of hydrolysis of the complexes when they are held at 100°C with a RH higher than 98% (100%, or condensed water that attack the metal centers). The powder XRD data in figure 6 suggest that the powder samples after proton-conductive measurement have the same supramolecular frameworks as those of **1** and **2**. The proton conductivities of **1** and **2**

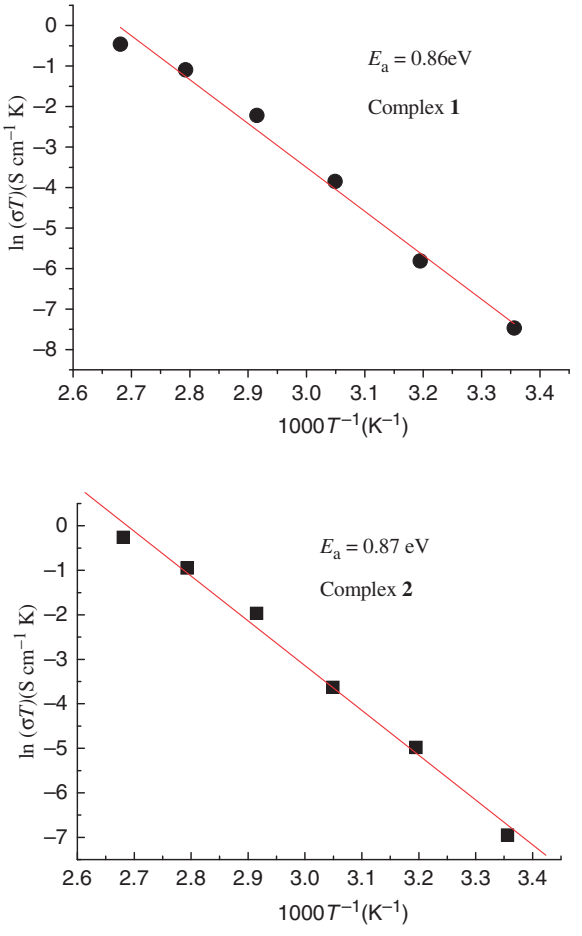

Figure 7. The Arrhenius plots of the proton conductivities of **1** and **2**.

were also measured at 70°C and 100°C in the RH range 35–98% by a complex-plane impedance method. Figure 8 shows the log σ (S cm^{-1}) *versus* RH plots of the complexes at 70°C and 100°C under 35–98% RH. The conductivities increase with RH at both the temperatures. As shown in figure 8, at 35% RH, conductivities of the complexes at 100°C are higher than those at 70°C. Yet, the TG analyses results clearly show the onset of water loss below 100°C. The results of measurement of the proton conductivity of the free HINO molecules at 70°C and 100°C at 35% RH showed that the free HINO molecules reached proton conductivities of 10^{-5} and 10^{-4} S cm^{-1}, which are similar to those of **1** and **2**. So, at 35% RH, conductivities of the complexes at 100°C being higher than those at 70°C may be mainly a result of dissociation of organic acid.

For **1** and **2**, although the M^{2+} ions are different, they have similar decorated poly-Keggin-anion chains, similar 3-D H-bonding networks, and proton conductivities, suggesting that the origin of proton conduction in these complexes is based on the self-ordered H-bonding structure, the orthorhombic space group *P*nnm, and the very close unit cell parameters.

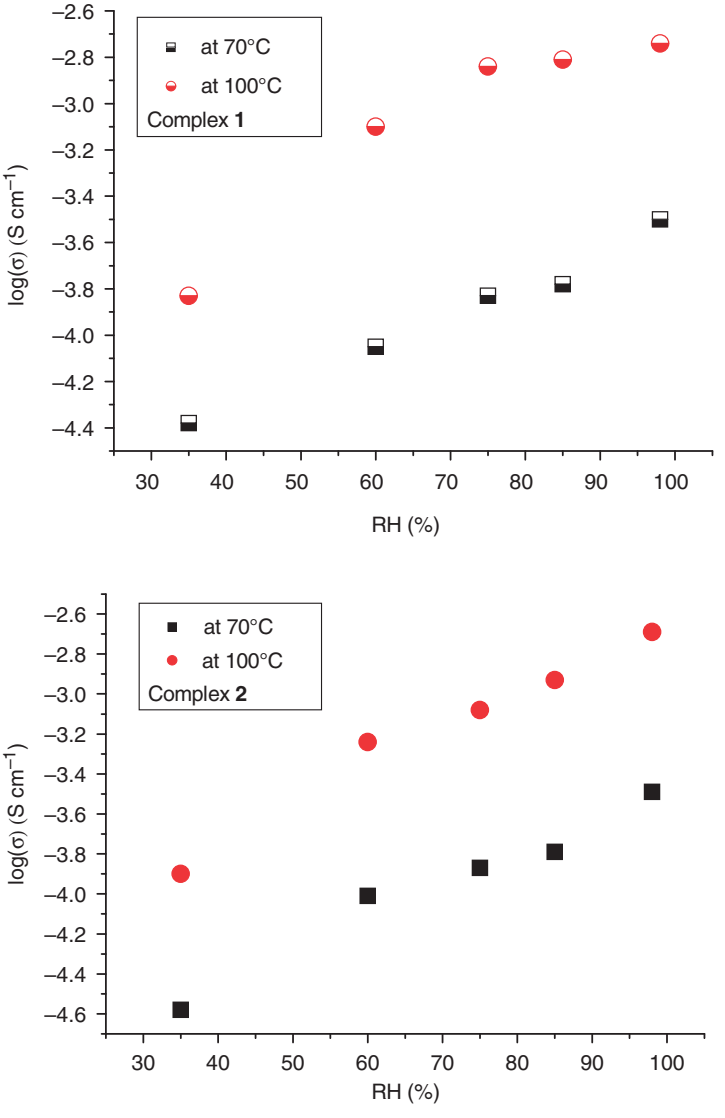

Figure 8. log σ (S cm^{-1}) *vs.* RH plots of **1** and **2** at 70°C and 100°C.

4. Conclusions

Two proton-conductive organic–inorganic complexes based on decorated poly-Keggin-anion chains and HINO molecules have been constructed. The organic–inorganic hybrid matrix changed the environment around the alkaline-earth metal salts of HPAs and influenced the formation of decorated poly-Keggin anions within the resultant structure. Thus, these complexes provide a new route to increase the stability and proton conductivity of organic–inorganic hybrid materials based on alkaline-earth metal salts of HPAs at high temperature.

Supplementary material

CCDC-846247 (for **1**) and CCDC-846248 (for **2**) contain the supplementary crystallographic data for this article. These data can be obtained free of charge from The Cambridge Crystallographic Data Centre *via* www.ccdc.cam.ac.uk/data_request/cif

Acknowledgments

This work was supported by the National Natural Science Foundation of China (Nos. 20971038 and 21171050) and the Natural Science Foundation of the Education Department of Henan Province (2009A150015).

References

[1] (a) B.C. Wood, N. Marzari. *Phys. Rev. B*, **76**, 134301 (2007); (b) R. Yu, L.C.D. Jonghe. *J. Phys. Chem. C*, **111**, 11003 (2007).
[2] K.D. Kreuer, S.J. Paddison, E. Spohr, M. Schuster. *Chem. Rev.*, **104**, 4637 (2004).
[3] O. Nakamura, T. Kodama, I. Ogino, Y. Miyake. *Chem. Lett.*, **8**, 17 (1979).
[4] M. Casciola, U. Constantino. *Solid State Ionics*, **20**, 69 (1986).
[5] (a) M. Misono. *Chem. Commun.*, 1141 (2001); (b) D.E. Katsoulis. *Chem. Rev.*, **98**, 359 (1998); (c) A.M. Herring. *Polym. Rev.*, **46**, 245 (2006).
[6] (a) G. Alberti, M. Casciola, U. Costantino, A. Peraio, T. Rega. *J. Mater. Chem.*, **5**, 1809 (1995); (b) X.G. Sang, Q.Y. Wu, W.Q. Pang. *Mater. Chem. Phys.*, **82**, 405 (2003); (c) I. Honma, S. Nomura, H. Nakajima. *J. Membr. Sci.*, **185**, 83 (2001).
[7] (a) Y.S. Kim, F. Wang, M. Hickner, T.A. Zawodzinski, J.E. McGrath. *J. Membr. Sci.*, **212**, 263 (2003); (b) J.L. Malers, M.A. Sweikart, J.L. Horan, J.A. Turner, A.H. Herring. *J. Power Sources*, **172**, 83 (2007).
[8] (a) V. Ramani, H.R. Kunz, J.M. Fenton. *J. Membr. Sci.*, **232**, 31 (2004); (b) A.M. Herring. *Polym. Rev.*, **46**, 245 (2006); (c) A. Verma, K. Scott. *J. Solid State Electrochem.*, **14**, 213 (2010).
[9] (a) J.D. Kim, I. Honma. *Solid State Ionics*, **176**, 547 (2005); (b) M.Q. Li, Z.G. Shao, K. Scott. *J. Power Sources*, **183**, 69 (2008); (c) A. Verma, K. Scott. *J. Solid State Electrochem.*, **14**, 213 (2010).
[10] (a) M.L. Wei, C. He, Q.Z. Sun, Q.J. Meng, C.Y. Duan. *Inorg. Chem.*, **46**, 5957 (2007); (b) M.L. Wei, C. He, W.J. Hua, C.Y. Duan, S.H. Li, Q.J. Meng. *J. Am. Chem. Soc.*, **128**, 13318 (2006); (c) C.Y. Duan, M.L. Wei, D. Guo, C. He, Q.J. Meng. *J. Am. Chem. Soc.*, **132**, 3321 (2010); (d) M.L. Wei, H.Y. Xu, R.P. Sun. *J. Coord. Chem.*, **62**, 1989 (2009); (e) M.L.Wei, R.P. Sun, K. Jiang, L. Yang. *J. Coord. Chem.*, **61**, 3800 (2008); (f) M.L. Wei, P.F. Zhuang, H.H. Li, Y.H. Yang. *Eur. J. Inorg. Chem.*, 1473 (2011); (g) M.L. Wei, P.F. Zhuang, Q.X. Miao, Y. Wang. *J. Solid State Chem.*, **184**, 1472 (2011); (h) M.L. Wei, P.F. Zhuang, J.H. Wang, X.X. Wang. *J. Mol. Struct.*, **995**, 51 (2011); (i) C.J. Zhang, H.J. Pang, D.P. Wang, Y.G. Chen. *J. Coord. Chem.*, **63**, 568 (2010); (j) Y.Z. Fu. *J. Coord. Chem.*, **63**, 1856 (2010).
[11] C. Rocchiccioli-Deltcheff, M. Fournier, R. Franck, R. Thouvenot. *Inorg. Chem.*, **22**, 207 (1983).
[12] P.G. Simpson, A. Vinciguerra, J.V. Quagliano. *Inorg. Chem.*, **2**, 282 (1963).
[13] Q.Y. Wu, S.L. Zhao, J.M. Wang, J.Q. Zhang. *J. Solid State Electrochem.*, **11**, 240 (2007).
[14] *SMART and SAINT, Area Detector Control and Integration Software*, Siemens Analytical X-ray Systems, Inc., Madison, WI (1996).
[15] G.M. Sheldrick. *SHELXTL (Version 5.1), Software Reference Manual*, Bruker AXS, Inc., Madison, WI (1997).
[16] (a) L.J. Zhang, D.H. Xu, Y.S. Zhou, F. Jiang. *New J. Chem.*, **34**, 2470 (2010); (b) M. Du, C.P. Li, J.H. Guo. *CrystEngComm.*, **11**, 1536 (2009); (c) M.A.S. Goher, F.A. Mautmer. *J. Mol. Struct.*, **846**, 153 (2007); (d) L.P. Zhang, M. Du, W. Lu, T.C.W. Mak. *Polyhedron*, **23**, 857 (2004).
[17] F. Bartl, G. Deckers-Hebestreit, K. Altendorf, G. Zundel. *Biophys. J.*, **68**, 104 (1995).
[18] (a) Y. Kanda, K.Y. Lee, S. Nakata, S. Asaoka, M. Misono. *Chem. Lett.*, **17**, 139 (1988); (b) J. Yang, M.J. Janik, D. Ma, A. Zheng, M. Zhang, M. Neurock, R.J. Davis, C. Ye, F. Deng. *J. Am. Chem. Soc.*, **127**, 18274 (2005).

[19] (a) K.D. Kreuer, S.J. Paddison, E. Spohr, M. Schuster. *Chem. Rev.*, **104**, 4637 (2004); (b) R.C.T. Slade, A. Hardwick, P.G. Dickens. *Solid State Ionics*, **9**, 1093 (1983); (c) G. Alberti, M. Casciola. *Solid State Ionics*, **145**, 3 (2001).
[20] (a) M.J. Janic, R.J. Davis, M. Neurock. *J. Am. Chem. Soc.*, **127**, 5238 (2005); (b) E.G. Hayashi, J.B. Moffat. *J. Catal.*, **83**, 192 (1983); (c) I. Honma, S. Nomura, H. Nakajima. *J. Membr. Sci.*, **185**, 83 (2001).
[21] K.D. Kreuer, A. Rabenau, W. Weppner. *Angew. Chem. Int. Ed.*, **21**, 208 (1982).
[22] (a) M. Sadakiyo, T. Yamada, H. Kitagawa. *J. Am. Chem. Soc.*, **131**, 9906 (2009); (b) W.A. England, M.G. Cross, A. Hamnett, P.J. Wiseman, J.B. Goodenough. *Solid State Ionics*, **1**, 231 (1980).
[23] N. Agmon. *Chem. Phys. Lett.*, **244**, 456 (1995).